Diffusion effects on the CPMG relaxation rate in a dipolar field

C.H. Ziener [a,*], T. Kampf [a], P.M. Jakob [a,b], W.R. Bauer [c]

[a] Julius-Maximilians-Universität Würzburg, Lehrstuhl für Experimentelle Physik 5, Am Hubland, 97074 Würzburg, Germany
[b] Research Center Magnetic-Resonance-Bavaria, Am Hubland, 97074 Würzburg, Germany
[c] Julius-Maximilians-Universität Würzburg, Medizinische Klinik und Poliklinik I, Oberdürrbacher Straße 6, 97080 Würzburg, Germany

ARTICLE INFO

ABSTRACT

The diffusion in the magnetic dipolar field around a sphere is considered. The diffusion is restricted to the space between two concentric spheres, where the inner sphere is the source of the magnetic dipolar field. Analytical expressions for the CPMG transverse relaxation rate as well as the free induction decay and the spin echo time evolution are given in the Gaussian approximation. The influence of the inter-echo time is analyzed. The limiting cases of small and large inter-echo times as well as the short and long time behavior are evaluated.

1. Introduction

In NMR experiments the signal is strongly influenced by the dephasing of spins in local inhomogeneous magnetic fields. To measure the transverse relaxation time without the effects of the local inhomogeneous fields the dephasing can be refocused using spin echoes. If diffusion in the local inhomogeneous magnetic field is not negligible, the signal can only be refocused partially. Therefore it is necessary to study the influence of the diffusion effects on the spin echo relaxation time.

To describe MR signal behavior in the presence of contrast agents [1], magnetically labeled cells [2] or alveolus of the lung [3–6] in an external magnetic field the model of a single sphere surrounded by a spherical dephasing volume is widely used. The implications of this model which is adapted from Krogh's capillary model [7] are described in detail in [8]. To understand the nature of the relaxation processes involved in contrast generation by nanoparticles, we analyze the CPMG relaxation rate, free induction decay and the time evolution of a spin echo in dependence on the relevant parameters.

Since the dipolar field is the first term of the multipolar expansion of the local inhomogeneous magnetic field, it is reasonable to consider the diffusion in a dipolar field. Such a dipolar field can be created by a homogeneous magnetized sphere with radius R_S. The diffusion of the spins occurs in the surrounding medium between the surface of the sphere and an outer boundary which is also assumed to be spherical. The dephasing volume is the space between the two concentric spheres with the radii R_S and R. The volume fraction is $\eta = R_S^3/R^3$.

According to the Larmor relation the resonance frequency of the surrounding spins is given by

$$\omega(\mathbf{r}) = \delta\omega R_S^3 \frac{3\cos^2\theta - 1}{r^3} = \delta\omega \underbrace{4\sqrt{\frac{\pi}{5}} Y_{20}(\theta, \phi)\left(\frac{R_S}{r}\right)^3}_{=f(\mathbf{r})}, \tag{1}$$

where $\delta\omega = \omega(r = R_S, \theta = \pi/2)$ is the resonance frequency on the equator of the sphere and characterizes the strength of the field inhomogeneity. The function $f(\mathbf{r})$ describes the geometry of the inhomogeneous field. It is worth noting that the resonance frequency in dipolar approximation depends on the spherical harmonic Y_{20} only.

2. Methods

The local inhomogeneous magnetic field induced by the magnetized sphere changes the dephasing of the surrounding water protons. This dephasing is normally refocused by a spin echo. However, diffusion hampers a complete refocusing of the spins resulting in a change in the apparent transverse relaxation time $T_2 = 1/R_2$ [9,10]. The measured R_2 relaxation rate consists of two parts: the intrinsic transverse relaxation rate $R_{2,0}$ and the second part ΔR_2 related to the diffusion of the nuclear spins in the dipolar field:

$$R_2 = R_{2,0} + \Delta R_2. \tag{2}$$

To describe the influence of second part ΔR_2, we use the weak field approximation proposed by Jensen and Chandra [11]. This approximation has the same structure as the approximation given by

Anderson–Weiss mean field theory [12–14]. In this approximation ΔR_2 can be expressed in terms of the correlation function $K(t)$ which characterizes the diffusion process in the local inhomogeneous field, and the inter-echo time τ_{180}:

$$\Delta R_2 = \frac{8}{\pi^2} \sum_{m=0}^{\infty} \frac{1}{(2m+1)^2} \int_0^{\infty} dt K(t) \cos\left[(2m+1)\pi\frac{t}{\tau_{180}}\right]. \quad (3)$$

In a recent work [15], it was demonstrated that the correlation function $K(t)$ can be expressed as a spectral expansion of the form

$$K(t) = \delta\omega^2 \sum_n F_n^2 e^{-\lambda_n^2 t/\tau}. \quad (4)$$

To characterize the diffusion process the correlation time [16]

$$\tau = \frac{R_S^2}{D}, \quad (5)$$

is introduced where D is the diffusion coefficient of the dephasing volume between the two concentric spheres. The eigenvalues λ_n obey the equation

$$j_2'(\lambda_n)y_2'\left(\frac{\lambda_n}{\sqrt[3]{\eta}}\right) = j_2'\left(\frac{\lambda_n}{\sqrt[3]{\eta}}\right)y_2'(\lambda_n), \quad (6)$$

where j_2 and y_2 are the spherical Bessel functions of second order. This equation must be solved numerically to find the appropriate eigenvalues in the spectral expansion. The expansion coefficients are derived in Appendix A and can be expressed by

$$F_n^2 = \frac{\frac{48\eta/(1-\eta)}{5j_2'(\lambda_n)y_2'(\lambda_n)}\left(y_2'(\lambda_n)\left[\eta T\left(\frac{\lambda_n}{\sqrt[3]{\eta}}\right) - T(\lambda_n)\right] - j_2'(\lambda_n)\left[\eta U\left(\frac{\lambda_n}{\sqrt[3]{\eta}}\right) - U(\lambda_n)\right]\right)^2}{\frac{y_2'(\lambda_n)}{j_2'(\lambda_n)}\left[V\left(\frac{\lambda_n}{\sqrt[3]{\eta}}\right) - V(\lambda_n)\right] + \frac{j_2'(\lambda_n)}{y_2'(\lambda_n)}\left[W\left(\frac{\lambda_n}{\sqrt[3]{\eta}}\right) - W(\lambda_n)\right] - 2\left[X\left(\frac{\lambda_n}{\sqrt[3]{\eta}}\right) - X(\lambda_n)\right]}, \quad (7)$$

where we introduced for abbreviation the functions $T(x)$, $U(x)$, $V(x)$, $W(x)$, and $X(x)$ which are given in Appendix A. For numerical evaluation of the correlation function, the Parseval-relation $\sum_{n=1}^{\infty} F_n^2 = \frac{4}{5}\eta$ can be used to estimate the number of required coefficients F_n. In the limit $\eta \to 1$ the dephasing volume tends to an infinitely thin shell. In this situation only the lowest eigenvalue $\lambda_1^2 = 6$ of the spectral expansion exists. This can be obtained from Eq. (6) by a Taylor expansion of the spherical Bessel functions. Therefore, in the limit $\eta \to 1$ the correlation function exhibits a purely mono-exponential decay determined by the first addend in Eq. (4) in the form $K(t) = \frac{4}{5}\delta\omega^2 \exp(-6t/\tau)$.

In the Gaussian approximation the free induction decay $M_{\text{FID}}(t)$ and the spin echo magnetization time signal evolution $M_{\text{SE}}(t)$ can be expressed in terms of the correlation function [17]

$$\frac{M_{\text{FID}}(t)}{M_{\text{FID}}(0)} = \exp\left(-\int_0^t d\xi(t-\xi)K(\xi)\right), \quad (8)$$

$$\frac{M_{\text{SE}}(t)}{M_{\text{SE}}(0)} = \exp\left(-\int_0^t d\xi(t-\xi)[K(\xi/2) - K(\xi)]\right). \quad (9)$$

These equations will be used to determine the signal evolution of the magnetization in a dipolar field.

3. Results

The spectral expansion of the correlation function in Eq. (4) can be used to determine the relaxation rate in Eq. (3). The integration is straightforward and yields the simple expression

$$\frac{\Delta R_2}{\tau\delta\omega^2} = \frac{8}{\pi^2} \sum_{m=0}^{\infty} \frac{1}{(2m+1)^2} \sum_{n=1}^{\infty} \frac{(F_n\lambda_n)^2}{\lambda_n^4 + (\pi(2m+1)\tau/\tau_{180})^2}. \quad (10)$$

With this expression in hand it is possible to analyze the influence of the inter-echo time τ_{180} on the relaxation rate ΔR_2. In Fig. 1 the
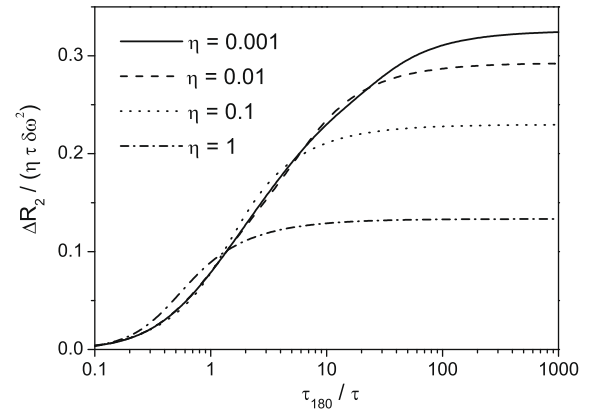

Fig. 1. Dependence of the CPMG relaxation rate on the inter-echo time obtained from Eq. (10).

dependence of the relaxation rate on the inter-echo time is visualized.

To verify the analysis above we compare the theoretical results with measurements of the inter-echo time dependence of the CPMG relaxation rate of human blood which were performed in [18]. The erythrocytes of the blood generate the resonance frequency $\delta\omega = \frac{4\pi}{3}\gamma\chi B_0$. The hematocrit of the blood corresponds to the volume fraction $\eta = 0.46$. We can fit Eq. (10) to the experimental results presented in Fig. 4a of [18] for deoxygenated blood (see Fig. 2) obtaining the parameters $\tau = 15.78$ ms, $\delta\omega = 154$ s^{-1} and the intrinsic relaxation rate $R_{2.0} = 8.62$ s^{-1} (see Eq. (2)). Assuming the diffusion coefficient $D = 2$ μm^2/ms the size of an erythrocyte follows from Eq. (5) to $R_S \approx 5.6$ μm. Since the experiments of Brooks et al. were performed at $B_0 = 1$ T we obtain the susceptibility $\chi \approx 0.14$ ppm. Although erythrocytes are not spherical at all we obtain a realistic value for the size of an erythrocyte. Our calculated value for the susceptibility of deoxygenated hemoglobin is similar to the value $\chi = 0.18$ ppm given in [19].

As discussed in Section 2, in the limit $\eta \to 1$ the correlation function exhibits a mono-exponential decay $K(t) = \frac{4}{5}\delta\omega^2 \exp(-6t/\tau)$ only. Since in this limit only the first expansion coefficient $F_1^2 = 4/5$ and the first eigenvalue $\lambda_1^2 = 6$ remains, we obtain from Eq. (10)

$$\lim_{\eta \to 1} \frac{\Delta R_2}{\tau\delta\omega^2} = \underbrace{\frac{48F_1^2}{\pi^2}}_{=\frac{192}{5\pi^2}} \underbrace{\sum_{m=0}^{\infty} \frac{1}{(2m+1)^2(36 + [\pi(2m+1)\tau/\tau_{180}]^2)}}_{=\frac{\pi^2}{864}\left[3 - \frac{\tau}{\tau_{180}}\tanh\left(3\frac{\tau_{180}}{\tau}\right)\right]} \quad (11)$$

$$= \frac{2}{15}\left[1 - \frac{1}{3}\frac{\tau}{\tau_{180}}\tanh\left(3\frac{\tau_{180}}{\tau}\right)\right], \quad (12)$$
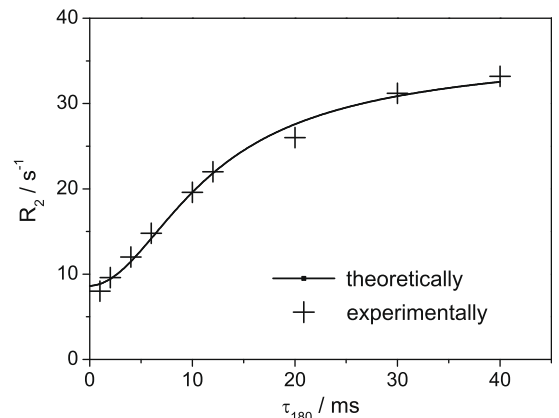

Fig. 2. Experimental results for deoxygenated blood (crosses) taken from the closed circles in Fig. 4a of [18]. The solid line is obtained from Eq. (10) with the parameters $\tau = 15.78$ ms and $\delta\omega = 154$ s^{-1}.

which has the form of the Luz–Meiboom exchange model [20]. For large inter-echo times the right hand side of Eq. (12) tends to $2/15 \approx 0.133$ (see Fig. 1 for $\eta = 1$ and large inter-echo times).

In the limit of large inter-echo times Eq. (10) tends to

$$\lim_{\tau_{180} \to \infty} \frac{\Delta R_2}{\tau \delta \omega^2} = \frac{8}{\pi^2} \underbrace{\sum_{m=0}^{\infty} \frac{1}{(2m+1)^2}}_{= \frac{\pi^2}{8}} \sum_{n=1}^{\infty} \frac{F_n^2}{\lambda_n^2} \approx \frac{16}{45} \eta, \qquad (13)$$

which corresponds to a mean relaxation time approximation. The expression $\sum F_n^2/\lambda_n^2$ is analyzed in Appendix B. As expected, in this limit the relaxation rate is independent on the inter-echo time for all volume fractions. In the limit $\tau_{180} \to \infty$ the CPMG sequence consists of the 90° pulse only. Therefore, the coherent part of the spin dephasing is not refocused and the obtained signal is the free induction decay. From Eq. (13) we obtain in this case the relaxation rate $\Delta R_2 = \frac{16}{45} \eta \tau \delta \omega^2$ which coincides with the results of Brooks, Moiny and Gillis [21]. It is worth noting that this relaxation rate is valid for the motional narrowing regime only. This is not surprising since the used Gaussian approximation is valid in the motional narrowing regime only. For $\eta = 1$ the exact solution of $\sum F_n^2/\lambda_n^2$ which is given in Eq. (B.4) tends to $2/15$. Thus, the limit for large inter-echo times is also in agreement with the long inter-echo time limit of the right hand side of Eq. (12).

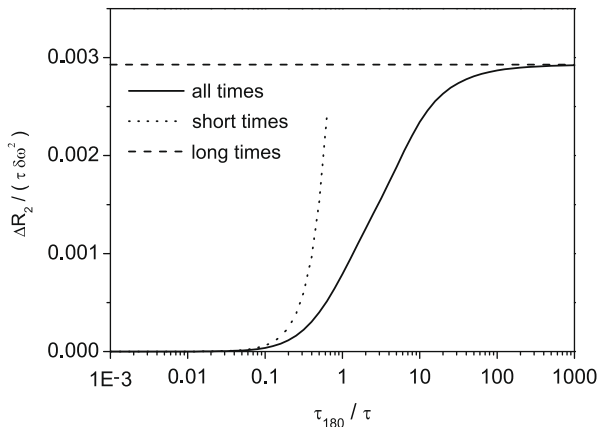In the opposite limit of small inter-echo times Eq. (10) tends to

$$\lim_{\tau_{180} \to 0} \frac{\Delta R_2}{\tau \delta \omega^2} = \frac{8}{\pi^4} \left(\frac{\tau_{180}}{\tau}\right)^2 \underbrace{\sum_{m=0}^{\infty} \frac{1}{(2m+1)^4}}_{= \frac{\pi^4}{96}} \sum_{n=1}^{\infty} F_n^2 \lambda_n^2, \qquad (14)$$

$$= \frac{3}{5} \left(\frac{\tau_{180}}{\tau}\right)^2 \eta \frac{\eta^{5/3} - 1}{\eta - 1}, \qquad (15)$$

$$\approx \frac{3}{5} \eta \left(\frac{\tau_{180}}{\tau}\right)^2, \qquad (16)$$

which exhibits a quadratic dependence on the inter-echo time: $\Delta R_2 \propto \tau_{180}^2$. The expression $\sum F_n^2 \lambda_n^2$ is analyzed in Appendix B. In Fig. 3 the limiting cases are visualized.

With the expansion (4) of the correlation function at hand it is straightforward to evaluate the integrals in Eqs. (8) and (9) and we finally obtain the time course of the magnetization for the free induction decay and the spin echo in Gaussian approximation:

$$\frac{M_{FID}(t)}{M_{FID}(0)} = \exp \left[-(\tau \delta \omega)^2 \sum_n F_n^2 \frac{\lambda_n^2 \frac{t}{\tau} + e^{-\lambda_n^2 \frac{t}{\tau}} - 1}{\lambda_n^4} \right], \qquad (17)$$

$$\frac{M_{SE}(t)}{M_{SE}(0)} = \exp \left[-(\tau \delta \omega)^2 \sum_n F_n^2 \frac{\lambda_n^2 \frac{t}{\tau} - e^{-\lambda_n^2 \frac{t}{\tau}} + 4e^{-\lambda_n^2 \frac{t}{2\tau}} - 3}{\lambda_n^4} \right]. \qquad (18)$$

For different volume fractions η the time dependence of $M_{FID}(t)$ is shown in Fig. 4 and for $M_{SE}(t)$ in Fig. 5.

The short time limit of Eqs. (17) and (18) can be given in terms of a Taylor expansion. We find

$$\lim_{t \to 0} \frac{M_{FID}(t)}{M_{FID}(0)} = \exp \left[-\frac{2}{5} \eta (\delta \omega t)^2 \right], \qquad (19)$$

$$\lim_{t \to 0} \frac{M_{SE}(t)}{M_{SE}(0)} = \exp \left[-\frac{3}{5} \eta \frac{\eta^{5/3} - 1}{\eta - 1} \delta \omega^2 \frac{t^3}{\tau} \right]. \qquad (20)$$

A similar asymptotic form of the short time limit has been obtained in [22].
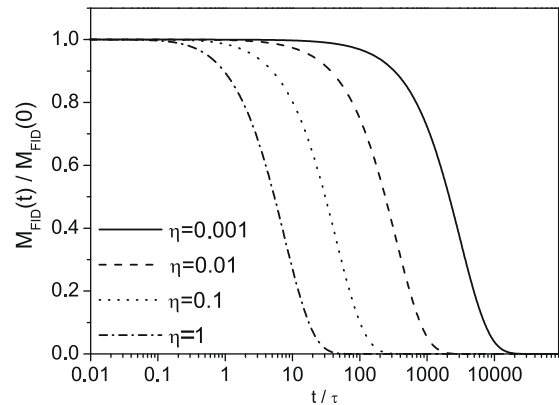
In the case of a linear gradient G Carr and Purcell [9] obtained for the signal attenuation of the CPMG sequence the expression

$$\frac{M(t)}{M(0)} = \exp \left[-\frac{t}{12} \gamma^2 G^2 D \tau_{180}^2 \right] = \exp[-\Delta R_2 t]. \qquad (21)$$
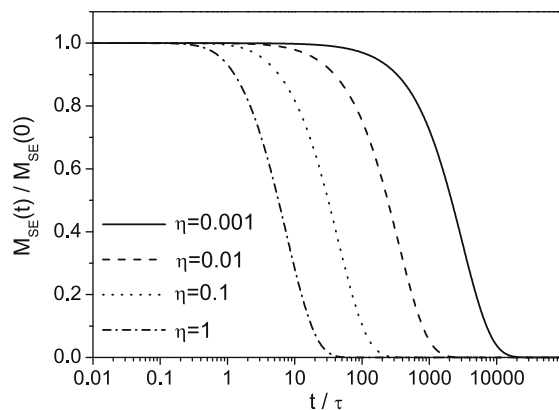
In a dipolar field the gradient is not constant. However, if we replace the constant gradient G by its averaged value in the form

$$\gamma^2 G^2 \to \frac{1}{V} \int_V d^3 \mathbf{r} [\nabla \omega(\mathbf{r})]^2 = \frac{36}{5} \frac{\delta \omega^2}{R_S^2} \eta \frac{\eta^{5/3} - 1}{\eta - 1}, \qquad (22)$$

it is possible to generalize the results of the linear gradient analysis. This replacement of the constant gradient by its averaged value is

Fig. 3. Limiting cases compared with the spectral expansion. For a volume fraction $\eta = 0.01$ the results of the spectral expansion obtained from Eq. (10) are shown in the solid line. In the limit of long inter-echo times the relaxation rate is independent on the inter-echo time (dashed line obtained from Eq. (13)). For short inter-echo times the relaxation rate exhibits a quadratic dependence on the inter-echo time (dotted line obtained from Eq. (15)).

Fig. 4. Magnetization decay obtained from Eq. (17) for $\tau \delta \omega = 1$.

Fig. 5. Magnetization decay obtained from Eq. (18) for $\tau \delta \omega = 1$.

justified for short inter-echo times, since in such a short time period between two echoes the gradient of the local resonance frequency remains nearly constant. Therefore, introducing Eq. (22) into Eq. (21) we obtain the previous result for short inter-echo times given in Eq. (15). In the case of a classical Hahn spin echo experiment ($t = \tau_{180}$) we obtain the previous result in Eq. (20). As expected the time dependence is analogous to the case of free diffusion.

In the long time limit the free induction decay as well as the spin echo converge to the same asymptotic form

$$\lim_{t\to\infty} \frac{M_{\text{FID}}(t)}{M_{\text{FID}}(0)} = \lim_{t\to\infty} \frac{M_{\text{SE}}(t)}{M_{\text{SE}}(0)} = \exp\left[-t\tau\delta\omega^2 \sum_n \frac{F_n^2}{\lambda_n^2}\right]$$
$$\approx \exp\left[-t\frac{16}{45}\tau\delta\omega^2\eta\right], \tag{23}$$

where the exact value of $\sum_n F_n^2/\lambda_n^2$ is given in Appendix B. As expected in the long time limit both values coincide. This results from the fact that for very long echo times the incoherent part of the spin dephasing that cannot be refocused by a spin echo dominates the time dependence. Furthermore, this is in agreement with result for the CPMG relaxation rate in the large inter-echo time limit in Eq. (13). The same results were obtained in [22].

4. Discussion

Based on a simple model of a spherical particle which generates a dipolar field we analyzed the CPMG relaxation rate as well as the time evolution of a free induction decay as well as the behavior of a spin echo in Gaussian approximation. For the CPMG relaxation rate we found an analytical expression in terms of a spectral expansion. This enables us to describe the dependence of the relaxation rate ΔR_2 on the inter-echo time τ_{180} tailored to an arbitrary exactness.

As can be seen from Fig. 1 the relaxation rate is proportional to the volume fraction for large inter-echo times and small volume fractions only. However, using the spectral expansion it is possible to give an analytical expression for the full parameter range, i.e. large volume fractions and arbitrary inter-echo times. For small volume fractions it can be seen from Eqs. (13) and (16) that the linear relation $\Delta R_2 \propto \eta$ is valid in the limit of short and long inter-echo times, which is in align with the results of [11,23].

Different limiting cases have been investigated and are in agreement with previously published results. Although the Luz–Meiboom exchange model was not intended to describe the MR signal in the situation examined in this analysis, we could show that in the case when the diffusion is restricted to the surface of a sphere this model yield the correct results.

Also for the free induction decay and the spin echo time evolution we were able to give analytical expressions exploiting the spectral expansion of the correlation function. As expected the time evolution of the CPMG sequence and the free induction decay coincide in the case that $\tau_{180} \to \infty$. In the short time limit both the free induction decay and the spin echo sequence exhibits the properties of free diffusion in a linear gradient. We could show that for short inter-echo times the previously obtained results for diffusion in a linear gradient can be generalized to a dipolar field by replacing the linear gradient by its expectation value in the sense of Eq. (22).

The present analysis is based on a magnetized sphere. If other geometries are considered, the geometry dependent function $f(\mathbf{r})$ in Eq. (1) changes only. Thus, the eigenvalues λ_n, the eigenfunctions $\psi_n(\mathbf{r})$ and the expansion coefficients F_n depend on the geometry and have to be evaluated using the geometry dependent function $f(\mathbf{r})$. However, the general form of the correlation function in Eq. (4) and the CPMG relaxation rate in Eq. (10) remains unaffected.

For example, in the case of cylinders with radius R_C the function $f(\mathbf{r}) = R_C^2 \cos(2\phi)/r^2$ has to be used [15]. In this case the dependence of the CPMG relaxation rate on the inter-echo time looks qualitatively similar to the spherical case shown in Fig. 1.

Acknowledgments

Appendix A. Spectral expansion of the correlation function

In this appendix, we give a brief summary about the calculation of the correlation function $K(t)$ in terms of a spectral expansion as demonstrated in [15]. The correlation function depends on the probability $p(\mathbf{r}, \mathbf{r}_0, t)$ for the transition of a spin between two local Larmor frequency $\omega(\mathbf{r})$ and the local Larmor frequency $\omega(\mathbf{r}_0)$ within a specific time t. Assuming a constant spin density between the two concentric spheres, the correlation function is given by [24]

$$K(t) = \frac{\delta\omega^2}{V} \int_V d^3\mathbf{r} \int_V d^3\mathbf{r}_0 \, f(\mathbf{r})p(\mathbf{r}, \mathbf{r}_0, t)f(\mathbf{r}_0), \tag{A.1}$$

where $f(\mathbf{r})$ describes the geometry of the dipolar field, while $\delta\omega$ characterizes its strength. Within this model this correlation function is the crucial quantity which has to be determined. The transition probability obeys the diffusion equation $\partial_t p(\mathbf{r}, \mathbf{r}_0, t) = D\Delta p(\mathbf{r}, \mathbf{r}_0, t)$, where D is the diffusion coefficient of the medium between the two concentric spheres. The diffusion equation can be solved via a spectral expansion [15]

$$p(\mathbf{r}, \mathbf{r}_0, t) = \sum_n e^{-\lambda_n^2 t/\tau} \psi_n(\mathbf{r})\psi_n(\mathbf{r}_0), \tag{A.2}$$

where the eigenfunctions $\psi_n(\mathbf{r})$ and eigenvalues $-\lambda_n^2$ obey the equation $\Delta\psi_n(\mathbf{r}) = -\frac{\lambda_n^2}{R_S^2}\psi_n(\mathbf{r})$. This spectral expansion (A.2) of the transition probability $p(\mathbf{r}, \mathbf{r}_0, t)$ can be introduced into expression (A.1). The sum over the eigenvalues in the spectral expansion can be extracted and we obtain for the correlation function the sum

$$K(t) = \delta\omega^2 \sum_n F_n^2 e^{-\lambda_n^2 t/\tau}, \tag{A.3}$$

with the expansion coefficients

$$F_n = \frac{1}{\sqrt{V}} \int_V d^3\mathbf{r} f(\mathbf{r})\psi_n(\mathbf{r}). \tag{A.4}$$

Due to the symmetry of the dipolar field only the index $n = 2$ remains and therefore the eigenfunctions simplify to the form

$$\psi_n(r, \theta, \phi) = \frac{1}{N_n}\left[y_2'(\lambda_n)j_2\left(\lambda_n \frac{r}{R_S}\right) - j_2'(\lambda_n)y_2\left(\lambda_n \frac{r}{R_S}\right)\right]Y_{20}(\theta, \phi). \tag{A.5}$$

On the surface of the inner and outer sphere reflecting boundary conditions are assumed. This is justified by the symmetry of the local resonance frequency $\omega(\mathbf{r}) = \omega(-\mathbf{r})$ and has been discussed in [15] in detail. Exploiting the reflective boundary conditions we obtain the eigenvalues λ_n with the help of Eq. (6). The normalization constant N_n results from the orthonormality of the eigenfunctions:

$$N_n^2 = R_S^3 \int_1^{\eta^{-1/3}} dz \, z^2 \left[y_2'(\lambda_n)j_2(\lambda_n z) - j_2'(\lambda_n)y_2(\lambda_n z)\right]^2. \tag{A.6}$$

To determine the coefficients F_n we introduce the eigenfunctions given in Eq. (A.5) in the definition of the expansion coefficients given in Eq. (A.4) and obtain

$$F_n = \frac{2}{N_n} \sqrt{\frac{3}{5} \frac{R_S^3 \eta}{1-\eta}} \int_1^{\eta^{-1/3}} \frac{dz}{z} \left[y_2'(\lambda_n) j_2(\lambda_n z) - j_2'(\lambda_n) y_2(\lambda_n z) \right]. \qquad (A.7)$$

The integration in Eqs. (A.6) and (A.7) is straightforward and yields Eq. (7). The abbreviations $T(x)$, $U(x)$, $V(x)$, $W(x)$, and $X(x)$ are given by

$$T(x) = x \cos x - \sin x,$$

$$U(x) = \cos x + x \sin x,$$

$$V(x) = \frac{1}{x^3} \left[2x^4 - 6(1+x^2) + 6(1-x^2)\cos 2x + x(12-x^2)\sin 2x \right],$$

$$W(x) = \frac{1}{x^3} \left[2x^4 - 6(1+x^2) + 6(x^2-1)\cos 2x + x(x^2-12)\sin 2x \right],$$

$$X(x) = \frac{1}{x^3} \left[x(x^2-12)\cos 2x + 6(1-x^2)\sin 2x \right].$$

$$(A.8)$$

Appendix B. Evaluation of $\sum F_n^2 / \lambda_n^2$ and $\sum F_n^2 \lambda_n^2$

To evaluate $\sum F_n^2 / \lambda_n^2$ in Eqs. (13) and (23) we consider the spectral expansion in Eq. (4) and find

$$\sum_{n=1}^{\infty} \frac{F_n^2}{\lambda_n^2} = \frac{1}{\tau \delta \omega^2} \int_0^{\infty} K(t) dt. \qquad (B.1)$$

To solve the integral it is advantageous to express the solution of the diffusion equation $\partial_t p(\mathbf{r}, \mathbf{r}_0, t) = D \Delta p(\mathbf{r}, \mathbf{r}_0, t)$ in the form $p(\mathbf{r}, \mathbf{r}_0, t) = e^{t D \Delta} \delta(\mathbf{r} - \mathbf{r}_0)$. Insertion of this probability density into the definition of the correlation function (A.1) results in

$$K(t) = \frac{\delta \omega^2}{V} \int_V d^3 \mathbf{r} f(\mathbf{r}) e^{t D \Delta} f(\mathbf{r}). \qquad (B.2)$$

Substitution of Eq. (B.2) in Eq. (B.1) yields

$$\sum_{n=1}^{\infty} \frac{F_n^2}{\lambda_n^2} = \frac{1}{V R_S^2} \int_V d^3 \mathbf{r} f(\mathbf{r}) \underbrace{\left[-\frac{1}{\Delta} \right] f(\mathbf{r})}_{=h(\mathbf{r})}, \qquad (B.3)$$

$$= \frac{2}{5} \frac{\eta}{1-\eta} \left[1 - \eta^{1/3} + \frac{4(1-\eta)^2 + 9(2\eta - \eta^{5/3} - \eta^{1/3})}{36(\eta^{5/3} - 1)} \right], \qquad (B.4)$$

where $h(\mathbf{r})$ in Eq. (B.3) obeys the relation $\Delta h(\mathbf{r}) = -f(\mathbf{r})$. The solution of this differential equation can be found in [16].

To evaluate $\sum F_n^2 \lambda_n^2$ in Eq. (14) we also consider the spectral expansion in Eq. (4) and find in analogy to the case above:

$$\sum_{n=1}^{\infty} F_n^2 \lambda_n^2 = -\frac{\tau}{\delta \omega^2} \frac{d}{dt} K(t) \Big|_{t=0}, \qquad (B.5)$$

$$= \frac{R_S^2}{V} \int_V d^3 \mathbf{r} [\nabla f(\mathbf{r})]^2, \qquad (B.6)$$

$$= \frac{36}{5} \eta \frac{\eta^{5/3} - 1}{\eta - 1}, \qquad (B.7)$$

where the right hand side of Eq. (B.6) has been evaluated in [15].

References

[1] L.E. LaConte, N. Nitin, O. Zurkiya, D. Caruntu, C.J. O'Connor, X. Hu, G. Bao, Quantitation of T2' anisotropic effects on magnetic resonance bone mineral density measurement, J. Magn. Reson. 26 (2007) 1634–1641.

[2] C.H. Ziener, W.R. Bauer, P.M. Jakob, Transverse relaxation of cells labeled with magnetic nanoparticles, Magn. Reson. Med. 54 (2005) 702–706.

[3] T.A. Case, C.H. Durney, D.C. Ailion, A.G. Cutillo, A.H. Morris, A mathematical model of diamagnetic line broadening in lung tissue and similar heterogeneous systems: calculations and measurements, J. Magn. Reson. 73 (1987) 304–314.

[4] C.H. Durney, J. Bertolina, D.C. Ailion, R. Christman, A.G. Cutillo, A.H. Morris, S. Hashemi, Calculation and interpretation of inhomogeneous line broadening in models of lungs and other heterogeneous structures, J. Magn. Reson. 85 (1989) 554–570.

[5] J.A. Bertolina, C.H. Durney, D.C. Ailion, A.G. Cutillo, A.H. Morris, K.C. Goodrich, Experimental verification of inhomogeneous line-broadening calculations in lung models and other inhomogeneous structures, J. Magn. Reson. 99 (1992) 161–169.

[6] A.G. Cutillo, Application of Magnetic Resonance to the Study of Lung, Futura Publishing, Armonk, New York, 1996.

[7] A. Krogh, The number and the distribution of capillaries in muscle with the calculation of the oxygen pressure necessary for supplying the tissue, J. Physiol. (Lond.) 52 (1919) 409–415.

[8] C.H. Ziener, T. Kampf, G. Melkus, V. Herold, T. Weber, G. Reents, P.M. Jakob, W.R. Bauer, Local frequency density of states around field inhomogeneities in magnetic resonance imaging: effects of diffusion, Phys. Rev. E 76 (2007) 031915.

[9] H.T. Carr, E.M. Purcell, Effects of diffusion on free precession in nuclear magnetic resonance experiments, Phys. Rev. 94 (1954) 630–638.

[10] S. Meiboom, D. Gill, Modified spin-echo method for measuring nuclear relaxation times, Rev. Sci. Instr. 29 (1958) 688–691.

[11] J.H. Jensen, R. Chandra, NMR relaxation in tissues with weak magnetic inhomogeneities, Magn. Reson. Med. 44 (2000) 144–156.

[12] R.P. Kennan, J. Zhong, J.C. Gore, Intravascular susceptibility contrast mechanisms in tissues, Magn. Reson. Med. 31 (1994) 9–21.

[13] P.W. Anderson, P.R. Weiss, Exchange narrowing in paramagnetic resonance, Rev. Mod. Phys. 25 (1953) 269–276.

[14] P.T. Callaghan, Principles of Nuclear Magnetic Resonance Microscopy, Oxford University Press, New York, 1991.

[15] C.H. Ziener, T. Kampf, V. Herold, P.M. Jakob, W.R. Bauer, W. Nadler, Frequency autocorrelation function of stochastically fluctuating fields caused by specific magnetic field inhomogeneities, J. Chem. Phys. 129 (2008) 014507.

[16] C.H. Ziener, W.R. Bauer, G. Melkus, T. Weber, V. Herold, P.M. Jakob, Structure-specific magnetic field inhomogeneities and its effect on the correlation time, Magn. Reson. Imaging 24 (2006) 1341–1347.

[17] A.L. Sukstanskii, D.A. Yablonskiy, Gaussian approximation in the theory of MR signal formation in the presence of structure-specific magnetic field inhomogeneities, J. Magn. Reson. 163 (2003) 236–247.

[18] R.A. Brooks, J. Vymazal, J.W.M. Bulte, C.D. Baumgarner, V. Tran, Comparison of T2 relaxation in blood, brain, and ferritin, J. Magn. Reson. Imaging 4 (1995) 446–450.

[19] E.M. Haacke, M.R. Thompson, R.W. Brown, R. Venkatesan, Magnetic Resonance Imaging: Physical Principles and Sequence Design, Wiley, New York, 1999.

[20] Z. Luz, S. Meiboom, Nuclear magnetic resonance study of the protolysis of trimethylammonium ion in aqueous solution—order of the reaction with respect to solvent, J. Chem. Phys. 39 (1963) 366–370.

[21] R.A. Brooks, F. Moiny, P. Gillis, On T2-shortening by weakly magnetized particles: the chemical exchange model, Magn. Reson. Med. 45 (2001) 10141020.

[22] A.L. Sukstanskii, D.A. Yablonskiy, Gaussian approximation in the theory of MR signal formation in the presence of structure-specific magnetic field inhomogeneities. Effects of impermeable susceptibility inclusions, J. Magn. Reson. 167 (2004) 56–67.

[23] J.H. Jensen, R. Chandra, H. Yu, Quantitative model for the interecho time dependence of the CPMG relaxation rate in iron-rich gray matter, Magn. Reson. Med. 46 (2001) 159165.

[24] C.H. Ziener, T. Kampf, G. Melkus, P.M. Jakob, W.R. Bauer, Scaling laws for transverse relaxation times, J. Magn. Reson. 184 (2007) 169–175.